

**August 31, 2005**

**MODELING OF GFR DECAY HEAT REMOVAL  
IN A DEPRESSURIZATION ACCIDENT**

**(ANNUAL REPORT FOR FY05)**

**Interim Report on GFR System Design and Safety**

**Lap-Yan Cheng  
Hans Ludewig**

**Submitted to DOE GEN-IV Program  
by  
Brookhaven National Laboratory**

## **1.0 INTRODUCTION**

This report summarizes the progress made in the modeling of decay heat removal for a 2400MW gas-cooled fast reactor (GFR) during FY05. The reactor system under consideration utilizes a closed helium Brayton cycle in its power conversion system. The reactor and the power conversion system are enclosed in a guard containment. The transient analysis of decay heat removal has been performed for a depressurization accident initiated by a postulated breach in the power conversion unit (PCU). Two passive decay heat removal mechanisms have been explicitly incorporated in the RELAP5/ATHENA model of the GFR. They are natural circulation and thermal radiation.

Owing to the coast down of the turbo-machine inside the PCU there is also a period of time during which forced flow cooling of the core is effective.

Decay heat removal by natural circulation cooling is enabled by an emergency cooling system (ECS) that directs the hot helium gas from the reactor to an ex-vessel heat exchanger. A dominant factor in determining the effectiveness of natural circulation cooling is the system pressure. A higher pressure results in a denser gas and that leads to a higher buoyancy head and subsequently a higher flow rate. In a depressurization accident initiated by a component breach the pressures of the reactor vessel and the guard containment will converge to an intermediate value. The impact of this common pressure on the maximum fuel temperature has been evaluated parametrically as part of the study [1].

An alternate means to remove decay heat is via the reactor cavity cooling system (RCCS) that surrounds the reactor vessel. Core decay heat is transferred to the reactor vessel by conduction and radiation and the RCCS absorbs the thermal energy from the reactor vessel both directly by radiation and indirectly by convection from the guard containment atmosphere. The impact of the RCCS on the guard containment atmosphere and the maximum fuel temperature has been examined as part of this study also [2].

An integral part of the transition from forced flow to natural circulation is the dynamic behavior of the turbo-machinery of the PCU. This report also describes the progress in the modeling of the different components of a PCU that will become part of the ATHENA model of the GFR plant system [3].

The following description of the ATHENA model of the GFR represents progress made during FY05. Details of the models and results of the calculations can be found in the interim reports [1,2,3].

## **2.0 REACTOR and EMERGENCY COOLING SYSTEM**

An ATHENA model of the reactor system has been constructed to address different parametric effects that influence the steady state and transient behavior of a 2400 MW pin core under natural circulation cooling at decay heat power levels [1]. The model consists of two power conversion system loops, an emergency heat exchanger loop with

its heat sink, and a guard containment surrounding the primary system. The two power conversion system loops consists of one and three PCU's respectively. The loop with a single PCU (600MW) is used to model the breach that causes the depressurization. The other loop is a lumped representation of the remaining three PCU's. This arrangement is shown schematically in Figure 1.

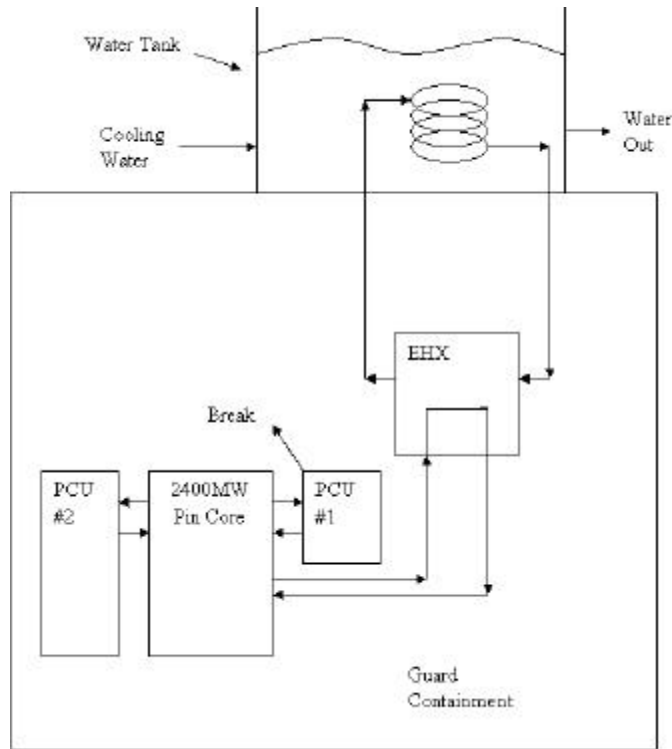


**Figure 1 – GFR System with Emergency Cooling Loop.**

## 2.1 Hydraulic Volumes and Heat Structures

The ATHENA model of the GFR consists of two basic building blocks, hydraulic volumes representing flow channels for the helium and heat structures representing solid components with internal heat generation and/or thermal capacity and resistance. Hydraulic volumes of the primary system and the power conversion unit (PCU) are shown in Figure 2. It is seen that all the components of the power conversion unit are represented. However, at this stage the actual turbine, compressors, generator models and heat exchangers are not complete. The actual models for these components, including performance maps and inertia terms, will be added at a later date. The detail modeling of the PCU components is discussed in a later section.

Several volumes are used to represent the core and the pressure vessel. The fuel and metal components are represented as heat structures. Details of the heat structures used in the ATHENA model for convective and radiative heat transfer are shown in Figure 3.

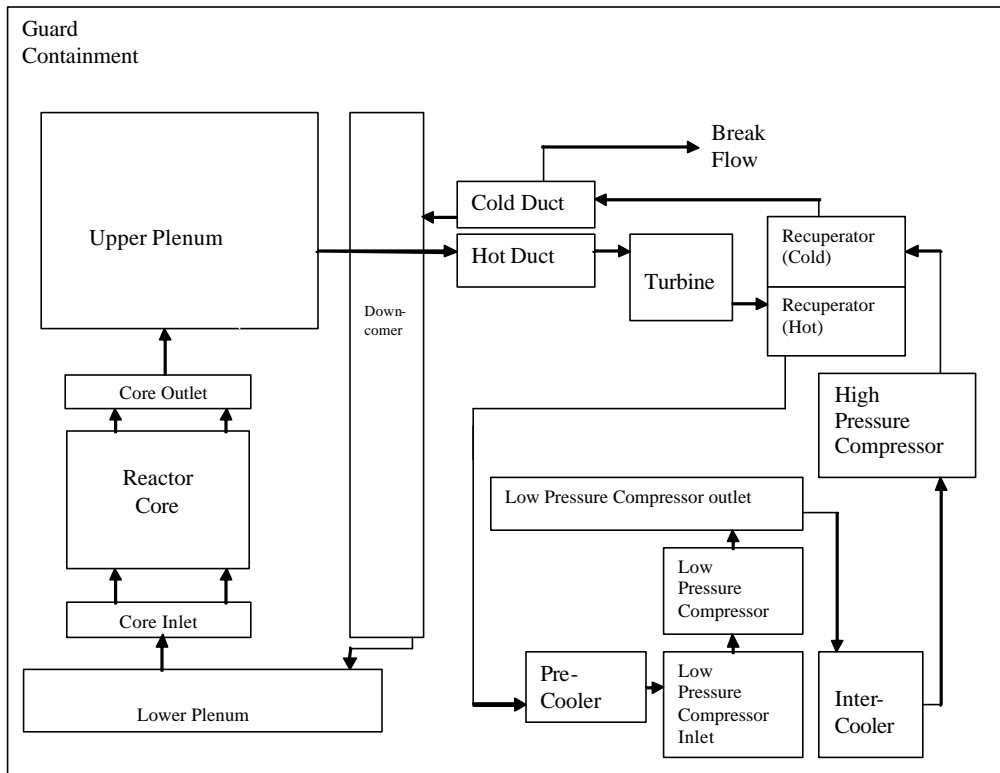


**Figure 2 – Reactor Vessel and Power Conversion Unit Volume Arrangement.**

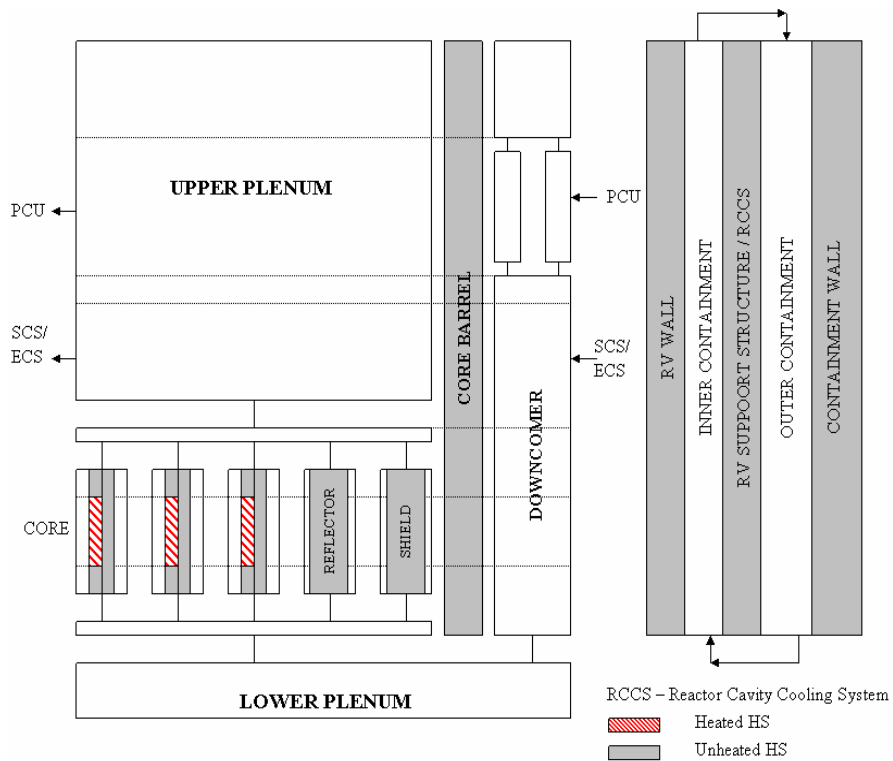


**Figure 3 – Reactor Vessel and Guard Containment Heat Structures.**

The core model consists of three radial zones and ten axial zones. The three radial zones include a hot assembly, a hot zone, and an average zone. Each of the radial zones is divided into ten axial zones. Power generation in each zone is obtained from output of the reactor physics analysis. Beyond the core there is a radial reflector, shield, core barrel, reactor pressure vessel wall and support structure, and finally the guard containment wall. It is noted that explicit heat generation is only modeled in the core volumes. Heat generation in the other volumes is of marginal importance, and these structures act only as thermal capacitors.

## 2.2 Radiative Heat Transfer

Radiative heat transfer is modeled between the heat structures [1]. Shown in Figure 4 is the conceptual arrangement of heat structures involved in the heat transfer by radiation.

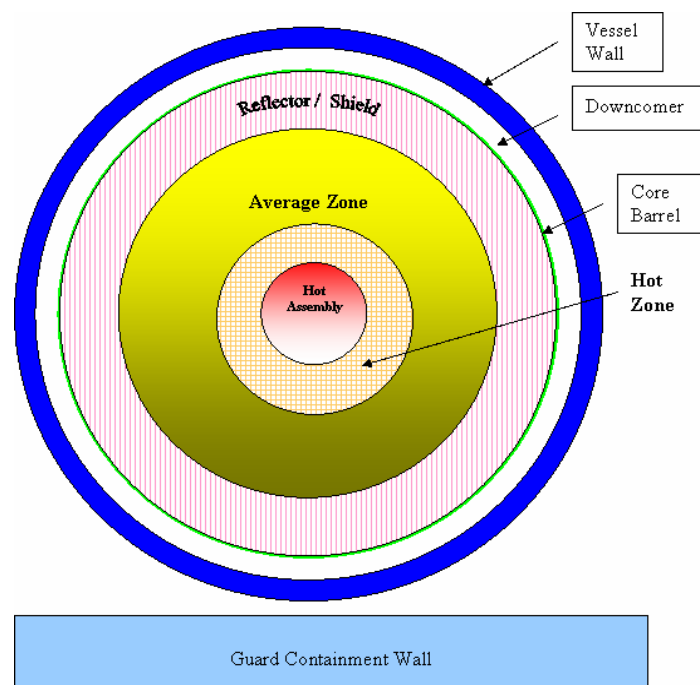


**Figure 4 – Heat Structures for Radiative Heat Transfer.**

This model allows for radial radiation heat transfer only, and couples the hot inner core parts to the cooler outer parts. Figure 4 is thus a radial section through the core and associated guard containment wall, since these are the heat structures involved in the heat transfer process. It is seen that the fuel pins radiate to the assembly cans, which in turn radiate to each other. At the outer core boundary the element cans radiate to the inner reflector surface, which radiates to the radial shield. Finally the shield radiates to the core barrel, which radiates to the reactor pressure vessel, and it finally radiates to the guard containment wall. It is assumed that the guard containment wall is kept at a constant temperature by a thermal management system embedded in the wall.

It is clear from the above discussion that the core heat transfer model has both a convective and a radiative component. Convectively, heat is removed from the core by helium gas flowing up along the fuel pins. This mechanism is either forced or natural convection. The second heat transfer mechanism is radiation from the hotter parts of the core to the cooler parts of the core.

### 2.3 Emergency Cooling System

During natural circulation, thermal energy is removed from the helium via the shutdown and emergency cooling system that is sized to handle 2% decay heat removal by natural convection in a 4x50% configuration, i.e. four separate loops of 1% power capacity. In the ATHENA model the emergency heat removal system is represented by one heat exchanger, which is sized to handle 2% of full power. Thus, once the decay heat reaches a level of 2 % of full power the emergency heat removal system should be able to handle the heat load. Details of the volume representation of the Shutdown Cooling System/Emergency Cooling System (SCS/ECS) are shown in Figure 5. The intermediate

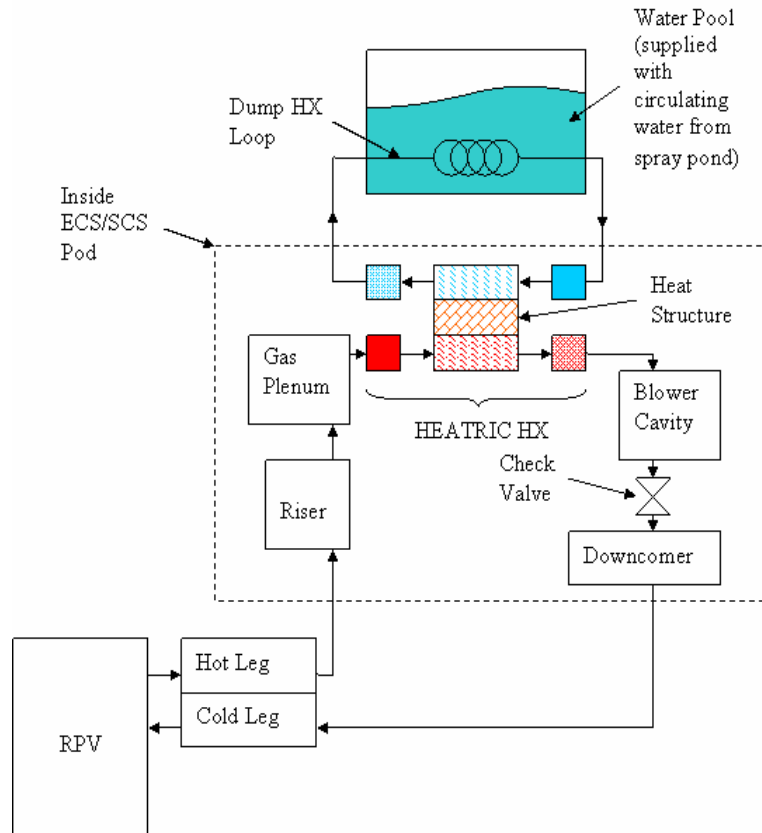


**Figure 5 – Schematic of Shutdown Cooling System/Emergency Cooling System.**

heat exchanger is based on the HEATRIC concept. The ultimate heat sink of the SCS/ECS consists of a large water tank located outside the guard containment building. The inlet and outlet of the SCS/ECS loop is connected to the upper plenum and the

downcomer of the reactor pressure vessel respectively. Although the blower volume is explicitly modeled, the actual blower rotating components are not included at this stage. The inertia of the drive motor and/or the possible availability of backup battery power both of which could assist in forcing coolant to circulate around the primary circuit are thus not included in this analysis.

For this analysis the emergency heat exchanger system is modeled after an MIT design [1], shown in Figure 6. The HEATRIC heat exchanger consists of alternating layers of helium and pressurized water counter-current micro-channels. The HEATRIC heat exchanger is represented in the ATHENA model as a plate heat structure separating the counter-current primary and secondary fluids. In Figure 5 the heat exchanger is shown in the horizontal orientation. However initial calculations showed a period of steam void formation at the start of heat transfer to the water side. Thus, for the calculations presented in this report the flow channels were oriented vertically to ease the establishment of natural circulation flow on the water side. The secondary heat exchanger, located in the ultimate heat sink, consists of a tube and shell design with ten tube passes and one shell pass. The shell side is a water tank that represents an ultimate heat sink. The tank is assumed to be very large, and if necessary can be refilled. The arrangement of the SCS/ECS heat exchanger as it is located in a pod in the guard containment is shown in Figure 6.

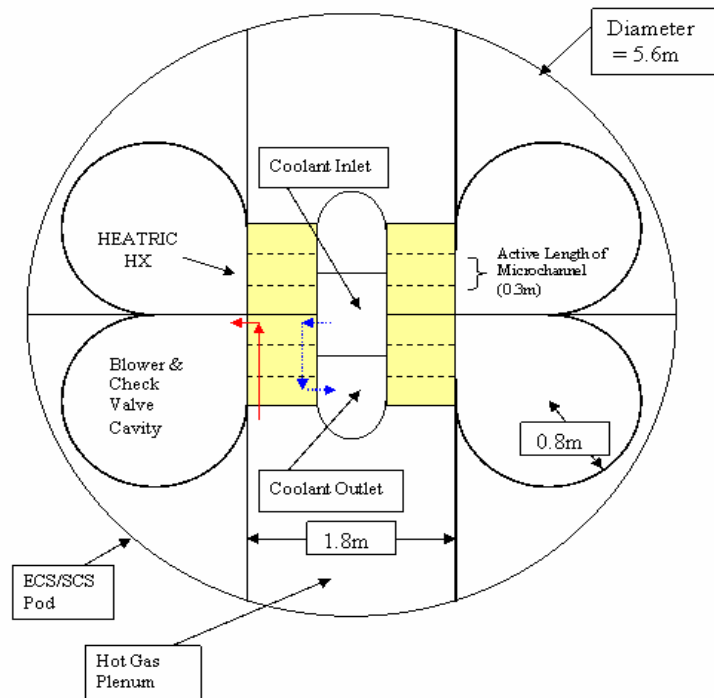


**Figure 6 – Schematic of SCS/ECS Heat exchanger Located in a Pod within the Guard Containment.**

### 3.0 REACTOR CAVITY COOLING SYSTEM

The reactor cavity cooling system (RCCS) is assumed to be an active system that absorbs radiant heat from the reactor vessel and removes heat from the guard containment atmosphere by natural convection. The ATHENA model of the guard containment has been modified by adding heat structures and hydraulic volumes to represent the RCCS and the new system replaces the heat structure in the previous model that represented the reactor vessel support structure [2]. The heat structures used in the ATHENA model for convective and radiative heat transfers are shown in Figure 3. The heated heat structures (HS), i.e. the fuel pins, identified in Figure 3 are the source of energy and the unheated heat structures are other components that participate in the exchange of thermal energy by radiation. For the radiative heat transfer model implemented in Section 2 of this report the zone of influence of radiative heat transfer is assumed to be confined to the cylindrical section that coincides with the vertical extent of the fueled region of the core. As an example, even though the core barrel (also, the reactor vessel wall, and the reactor vessel support structure) extends to the upper plenum, only the lower portion between the lower and upper boundaries of the fueled zone (1.347m in height) participates in radiative heat transfer. This assumption is relaxed in the current analysis to accommodate the RCCS that spans the entire height of the reactor vessel. In particular the entire core barrel now communicates radiatively with the full height of the reactor vessel wall and in turn the full height of the reactor vessel radiates to either the vessel support structure (old configuration) or the RCCS (new configuration).

The ATHENA model for the RCCS is based on a set of input developed at INL [4]. As shown in Figure 7 the RCCS is modeled with three cylindrical heat structures that are

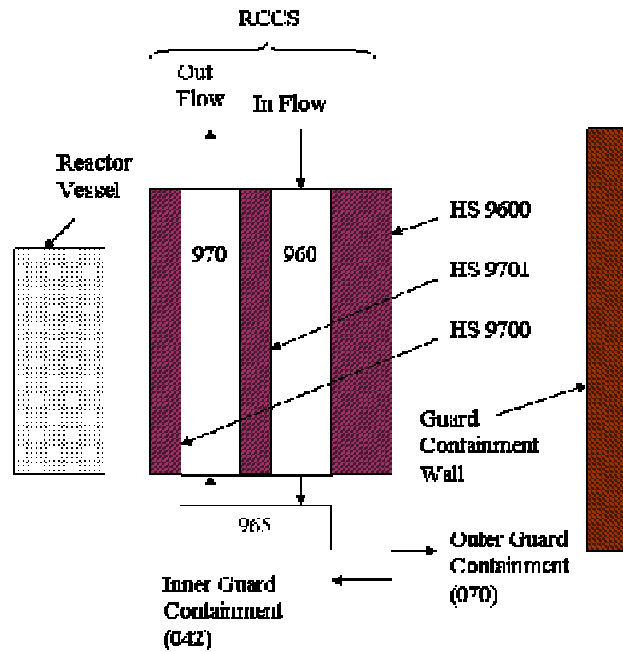


Figure 7 - ATHENA Model of the RCCS.



concentric with the reactor vessel. The inner wall (HS 9700), closest to the reactor vessel is followed by the interior wall (HS 9701) and the outer wall (HS 9600) respectively. The incoming (down flow) and outgoing (up flow) streams of cooling water are separated by the interior wall. The inner wall is made of stainless steel and has a wall thickness of 0.0127m. This wall is in contact with the inner guard containment volume (042) that occupies the part of the guard containment that is within the confine of the RCCS and also includes the region above the reactor and the RCCS. The interior wall of the RCCS is modeled with a 0.01746m thick structure of low conductivity material. The outer wall of the RCCS has two layers, a 0.0127m layer of stainless steel and a 1m thick wall of concrete. The concrete wall is in contact with the atmosphere of the outer guard containment volume (070). The inner and outer guard containment volumes are connected at the top and bottom to facilitate internal recirculation. The wall of the 44m high guard containment is modeled with a 0.02m concrete wall.

It is assumed in the ATHENA calculations that the outside surface of the guard containment wall is kept at a constant temperature of 30°C by a thermal management system embedded in the wall. The RCCS is assumed to be cooled by 30°C water and the flow is high enough to maintain the temperature rise to less than 1 deg. C. These two boundary conditions are set to maximize the cooling of the guard containment atmosphere by the containment wall and the RCCS.

#### **4.0 POWER CONVERSION UNIT**

It has been recognized from the results of initial analyses of the depressurization accident that the coolant flow due to the coast down of the turbo-machine of the power conversion unit (PCU) is an important factor in initially cooling the core following reactor scram, and in establishing the natural circulation flow. Currently this flow is approximated by linearly reducing the flow velocity to zero in 180 seconds. A more realistic model of this flow reduction (both mass flow rate and time) is required to make more accurate estimates of the maximum fuel temperature, and ultimately the guard containment volume. In order to carry out this more realistic calculation a complete PCU model is required. The following is a discussion of the progress made in the modeling of the PCU that will become part of the ATHENA model of the GFR plant system [3].

A node diagram showing the gas volumes in a PCU is shown in Figure 8. The power conversion unit (PCU) of interest is a design that is being developed by General Atomics (GA) and its Russian partner for a 600 MWt Gas Turbine-Modular Helium Reactor (GT-MHR). Conceptual design of the GT-MHR was done by GA and further development is being carried out in Russia with support from the US government. A PCU has two major parts, the turbo-machine and the heat exchangers. The components of a PCU are housed in a vertical vessel that is placed near the reactor. The PCU and the reactor are connected by a short cross vessel that is made up of an inner hot duct and a concentric outer cold duct. Components of the turbo-machine, namely, the generator, turbine, low and high pressure compressors, are all on one shaft. The heat exchangers consist of recuperator, precooler, and intercooler. A bypass valve that connects the high and low pressure side of the PCU is used for the over-speed protection of the turbine.

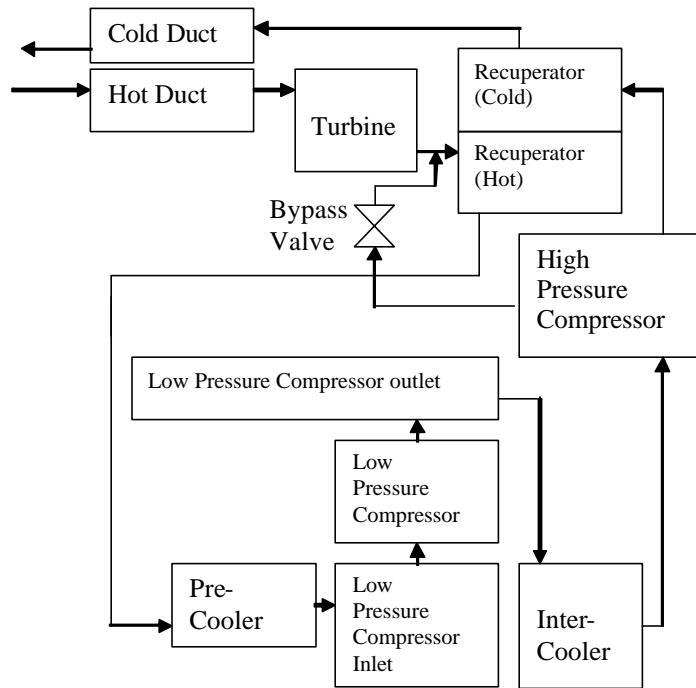


**Figure 8 – Node Diagram of Power Conversion Unit.**

Stand-alone ATHENA models of the turbine, compressors, recuperator, pre-cooler, and inter-cooler have been prepared. In general the predicted thermal capacities of the components are within a few percent of the values shown in Table 1.

**Table 1 – Helium State Points**

Component	Inlet Conditions	Outlet Conditions	Thermal Capacity
Turbine	848 °C 7.07 MPa	508 °C 2.61 MPa	558.5 MW
Recuperator (Low Pressure)	508 °C 2.61 MPa	130.3 °C 2.58 MPa	639 MW
Pre-cooler	130.3 °C 2.58 MPa	26.4 °C 2.55 MPa	173 MW
Low Pressure Compressor	26.4 °C 2.55 MPa	107.5 °C 4.31 MPa	132.3 MW
Inter-cooler	107.5 °C 4.31 MPa	26 °C 4.28 MPa	130.2 MW
High Pressure Compressor	26 °C 4.28 MPa	110.3 °C 7.24 MPa	134.5 MW
Recuperator (High Pressure)	110.3 °C 7.24 MPa	488 °C 7.16 MPa	639 MW

Since the performance data for the multi-stage turbine is not available, only an approximate ATHENA model is used to represent the gas turbine. It is modeled as a single stage type 2 turbine, i.e. constant efficient stage.

As the ATHENA model of a compressor has only recently been made available, in the interim approximate models are used to represent the low and high pressure compressors. The pump model is used as a surrogate for the compressor. In order to make full use of the compressor model in ATHENA, knowledge of the performance characteristics of the compressors is required.

Located in the annular space between the turbine-compressors and the PCU vessel are the recuperator, the precooler and the intercooler. The coolers are cooled by flowing water that transfers heat to the ultimate heat sink.

The recuperator is a vertical modular heat exchanger with plate-fin heat transfer surface and operating with countercurrent flow. The heat transfer coefficient calculated by ATHENA for a flat plate is adjusted by using the fouling factor input to achieve the desired heat transfer rate for a given flow and surface area.

The precooler and the intercooler have similar design. They are both modular vertical heat exchangers. Each module consists of a number of straight tubes with outer fins and the tubes are arranged in a triangular array. Cooling water flows inside the tubes. A displacer rod located inside each tube enhances the heat transfer by increasing the flow velocity. Helium flows on the outside of the tubes, countercurrent to the water flow.

## **5.0 RESULTS OF ANALYSIS**

Two series of transient calculations were done to exercise the modeling of decay heat removal in a GFR during a depressurization accident. In both series of calculations the reactor was at full power (2400 MW) when a  $0.00645\text{m}^2$  ( $1.0\text{ in}^2$ ) rupture in the #1 loop (see Figure 1) of the PCU cold leg initiated the transient.

### **5.1 Initial Results**

The first series of calculations utilizing the ATHENA model described in Section 2 was performed to evaluate the effect of guard containment pressure on the passive mode of decay heat removal by natural circulation cooling [1]. The effect of back pressure on natural circulation cooling of the pin core was evaluated by parametrically varying the free volume of the guard containment. The nominal case (Case 1) had an assumed guard containment volume of  $27000\text{ m}^3$  and a final calculated pressure of  $0.574\text{MPa}$ . The other cases had volumes and final pressures as shown in Table 2. Only two of the four cases, namely Case 2 and 4, resulted in an end state whereby natural circulation cooling has sufficient capacity to remove decay heat generated by the 2400 MW core. A natural circulation cooling transient was considered a success or adequate if the maximum fuel temperature in the hot channel remained less than  $1600^\circ\text{C}$  throughout the transient. Results from this first series of calculations indicate that the guard containment back

pressure has a dominant effect on the rate of heat removal by natural circulation, with a higher pressure leading to a higher flow rate.

**Table 2 – Summary of Initial Results**

Case Identification	Guard Containment Free Volume (m <sup>3</sup> )	Final Containment Pressure (MPa)	Maximum Fuel Temperature (°C)
Case 1	27000 (Nominal)	0.574	Exceeded 1600
Case 2	0.5 x Nominal	0.901	1001
Case 3	1.33 x Nominal	0.472	Exceeded 1600
Case 4	0.75 x Nominal	0.675	1464

The contribution of radiation heat transfer to the overall cooling of the fuel pins is demonstrated by the following tabulation (Table 3) that shows the energy balance for the upper half of the fuel pin in the hot assembly for Case 4 at the end of the calculation (24000s). In Table 3, the axial location of the mid-point of the heat structures representing the top half of the active fuel, is relative to the core mid-plane.

**Table 3 – Energy Balance for the Top Half of Fuel Pins in Hot Assembly**

Heat Structure Location	Loss by Radiation (W)	Loss by Convection (W)	Power Source (W)	Net Loss of Power (W)
0.15 (Node 550006)	12796	44351	56987	159.71
0.45 (Node 550007)	14102	38994	52931	165.25
0.725 (Node 550008)	11292	27168	38335	124.76
0.925 (Node 550009)	6362	14334	20629	67.159

The corresponding heat structure temperatures and the coolant temperatures are shown in Table 4. The above tabulation shows that radiation accounts for 20-30% of the power loss from the fuel pin in the hot assembly. Radiation heat transfer becomes less significant for heat structures as their distance from the hot assembly is increased. The presence of unheated heat structures inside the reactor vessel increases the heat capacity of the system and this also helps to lower the heat up of the helium gas inside the vessel.

**Table 4 – Temperatures in the Top Half of the Hot Assembly**

Heat Structure Location	Length of Node (m)	Fuel Temperature (°C)	HEX Can Temperature (°C)	Coolant Temperature (°C)
0.15 (Node 550006)	0.20205	1135	1106	1110
0.45 (Node 550007)	0.20205	1295	1270	1274
0.725 (Node 550008)	0.168381	1405	1385	1388
0.925 (Node 550009)	0.101029	1463	1446	1448

## 5.2 Results with RCCS

The second series of calculations was done with the addition of the RCCS [2]. These calculations were performed by using the same system model and the same depressurization accident as described in Section 5.1. With the modifications to the radiative heat transfer model for the core barrel, vessel wall, and vessel support structure, it becomes necessary to establish a new baseline analysis for use in comparison with the case of the RCCS. The new baseline case is similar to Case 4 described in Section 5.1. The depressurization accident is initiated by a 0.00645 m<sup>2</sup> (1.0 in<sup>2</sup>) rupture in the cold leg of one of the PCUs (4 loops of 600MW each). A guard containment free volume of 20250 m<sup>3</sup> is assumed and the initial pressure and temperature of the guard containment atmosphere are one atmosphere and 30°C respectively.

Two transient cases had been run, one with and one without the RCCS. The later is the new base case. The benefits of having the RCCS are evident in the guard containment conditions. Both the pressure and temperature of the guard containment are lower in the case with RCCS (Case 5) than the case without (Case 4a, the base case) it. The trend of lower temperature however does not extend to the peak fuel temperature Results of the two cases, at the end of a 24000s run, are summarized below.

**Table 5 – Summary of Results with RCCS**

Case Identification	Final Peak Fuel Temperature (°C)	Final Containment Pressure (MPa)	Final Containment Temperature (°C)
Case 4a (No RCCS, Base Case)	1321	0.658	82.
Case 5 (With RCCS)	1499	0.611	52.

It is noted that the maximum fuel temperature during the depressurization accident is only a few degrees different from the final peak fuel temperature shown in the above table. With a lower guard containment pressure, the natural circulation flow established in the reactor is correspondingly lower in the case with RCCS. This then leads to a higher peak fuel temperature in Case 5. The peak fuel temperature result demonstrates that the predominant mode of decay heat removal is by convection while radiative heat transfer only serves a minor role in heat dissipation from the fuel. For the purpose of comparison, at the initial steady-state reactor power of 2400MW, the RCCS removes about 2MW of power while the emergency cooling system (ECS) removes about 20MW of power from the reactor at the end of the calculation at 24000s.

It is noted that although Case 4a is the same transient as Case 4 in Section 5.1, the new analysis has a few modifications in the inputs for the heat structures. These changes resulted in a generally lower guard containment pressure and lower temperatures (fuel and guard containment) than before.

The progression of the depressurization transient for Case 4a and Case 5 is very similar. The following sections discuss the thermal-hydraulic response of some of the more important system parameters during the transient. For each system parameter the ATHENA results for both cases are plotted together to facilitate the comparison of the two cases.

### 5.2.1 Heat Removal Rate of the Emergency Cooling System

Plotted in Figure 9 is the rate of heat transfer into the water side of the HEATRIC heat exchanger in the emergency cooling system. The reactor power also is shown in the figure for comparison. The initial surge in the heat removal rate is due to the hydraulic

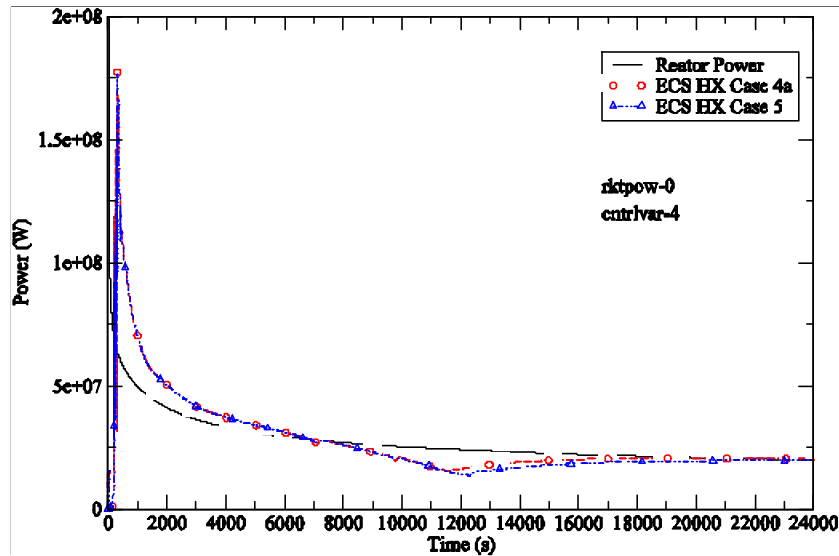


Figure 9 – Reactor Power and Emergency Heat Exchanger Heat Removal Rate.

transient on the water side of the heat exchanger as explained in [1]. A comparison between Figures 9, 10 and 11 shows that as the reactor pressure comes into equilibrium with the guard containment pressure, indicating an end to the depressurization phase of the transient, there is a slow migration of the heat exchanger heat removal rate towards the reactor power. This trend is indicative of the approach to a quasi-steady state where the natural circulation heat removal rate matches that of the reactor power.

### 5.2.2 Reactor Pressure

The pressure of the reactor upper plenum is shown in Figure 10. With the initiation of the break at time zero, the current RELAP5/ATHENA model assumes a linear coast down of the velocity from the power conversion unit (PCU) to the reactor. This is an interim scheme to simulate the behavior of a tripped PCU until a compressor/turbine model is developed for a more realistic representation of the PCU. The mean initial pressure of the PCU is less than the reactor pressure. With no rotating machinery in the current model to provide hydraulic head in the PCU, helium gas in the reactor quickly depressurizes into the PCU volumes. This results in a rapid drop in reactor pressure at time zero. The rest of the depressurization is more gradual and is due to leakage through the break into the guard containment. For much of the depressurization transient the helium flow through the leak is choked and thus both cases have similar reactor pressure until the point at which the reactor pressure equalizes with the guard containment pressure. It is noted that the blow down takes a little longer in Case 5 than Case 4a. The reason is a lower back pressure in the latter (see Figure 11).

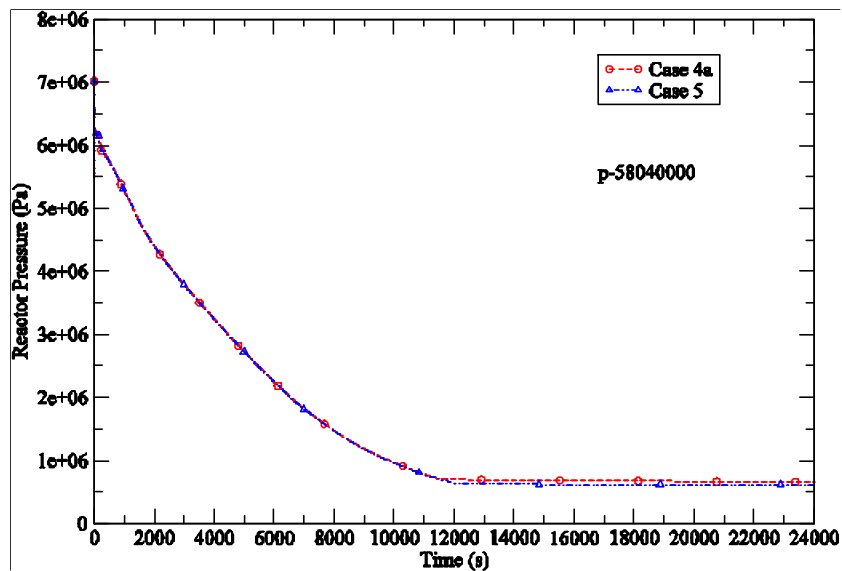


Figure 10 – Reactor Pressure in the Upper Plenum.

### 5.2.3 Guard Containment Pressure

There are several factors that determine the pressure build up in the guard containment after a leak in the reactor primary circuit. They are:

1. Initial state of the guard containment atmosphere, i.e. temperature, pressure, and volume.
2. Presence of heat structure to absorb sensible heat inside the guard containment.
3. Presence of active cooling device in the guard containment.
4. Through wall heat transfer to the outside.
5. Energy and mass transfer through the leak into the guard containment.

In Figure 11 the rate of pressure build up is seen to be faster for Case 4a than Case 5 and the former also has a higher containment pressure. A peak pressure is reached when the reactor and guard containment have reached the same pressure and the combined heat removal from the Emergency Cooling System, Reactor Cavity Cooling System, and heat conduction through the guard containment wall exceeds the decay power.

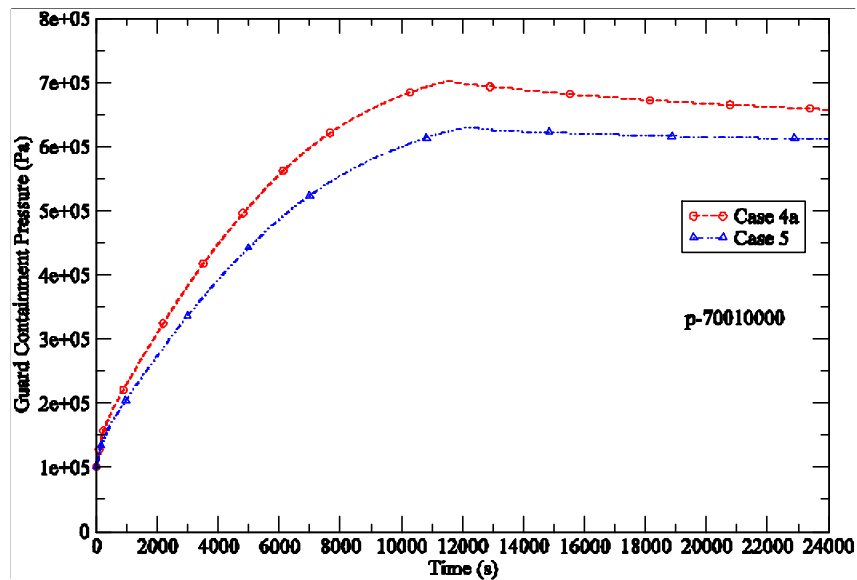


Figure 11 – Guard Containment Pressure.

### 5.2.4 Guard Containment Gas Temperature

The gas temperature of the guard containment increases rapidly after the initiation of the depressurization accident because of the relatively low heat capacity of its atmosphere. Figure 12 shows that the gas temperature is lower when the RCCS is included in the analysis. A high gas temperature is of concern not only for the environmental qualification of equipment and instruments inside the guard containment but also for the structural integrity of the support structures and the guard containment itself.



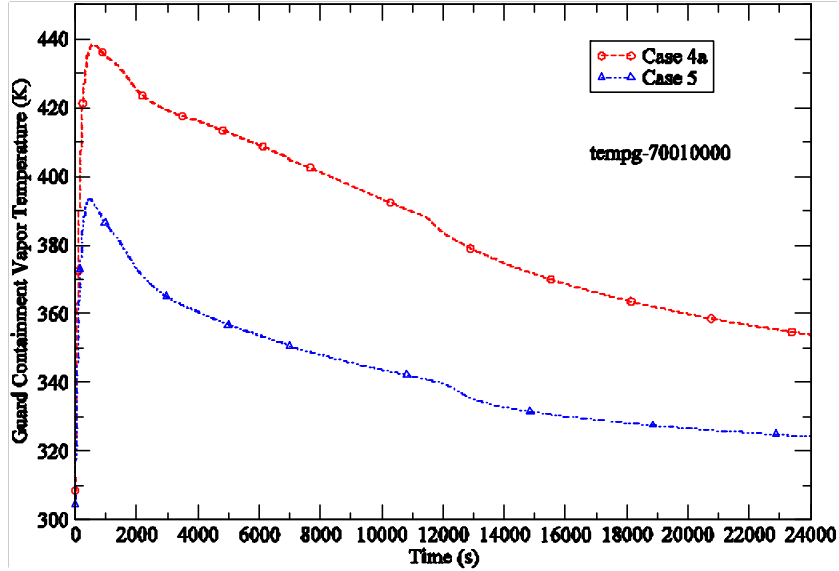


Figure 12 – Gas Temperature Inside the Guard Containment.

### 5.2.5 Peak Fuel Temperature

Figure 13 shows the peak fuel temperature as a function of time. It is obtained from the RELAP5/ATHENA results by defining a control variable that searches for the maximum temperature for all fuel heat structures at all axial locations. It is noted that there is little deviation between the peak fuel temperatures for the two cases until about 12000s

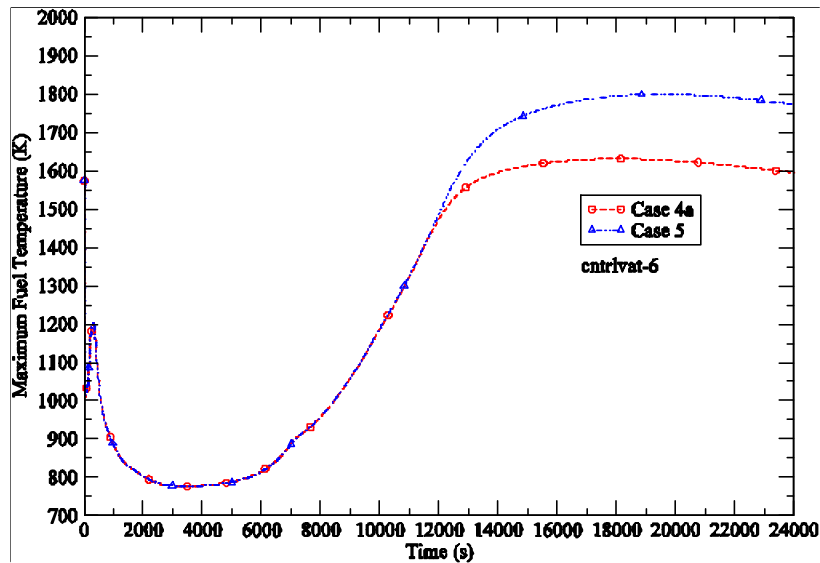


Figure 13 – Peak Fuel Temperature Core-wide.

when Case 4a has finished its blow down. Before that time the two cases have the same reactor pressure and almost the same natural circulation flow (see Figure 14). In both cases the maximum fuel temperature during the transient is within the success criterion of 1873K, with the RCCS case (Case 5) exhibiting a closer approach to the limit.

### 5.2.6 Helium Flow in Natural Circulation

Natural circulation flow is established when the pressure difference across the check valve in the emergency heat exchanger loop has reached a threshold value. The helium flow rate shown in Figure 14 clearly demonstrates its dependence on the reactor pressure (see Figure 10). Higher flow rates are achieved at higher pressures and that is the reason the base has a higher flow rate than the RCCS case when the system pressure has reached its quasi-steady state value. Based on economic and engineering constraints a maximum design pressure will be specified for the guard containment and that will have a direct bearing on the maximum passive heat removal rate achievable by natural circulation alone.

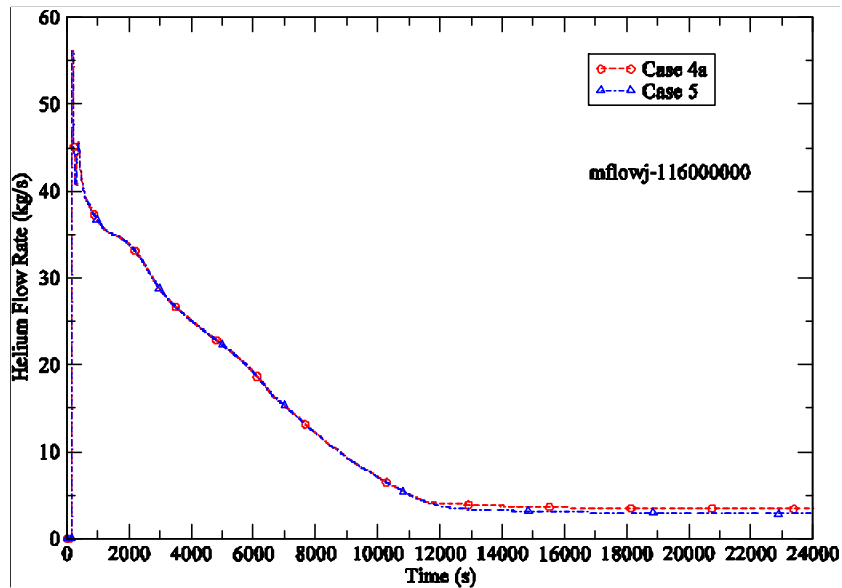


Figure 14 – Natural Circulation Flow Rate of Helium Gas.

### 5.2.7 Gas Temperature at Core Outlet

The gas temperature at the core outlet, shown in Figure 15, generally reflects the rate of heat transfer from the core to the helium flow. The progression of the core outlet temperature thus follows the trend of the fuel temperature shown in Figure 13.

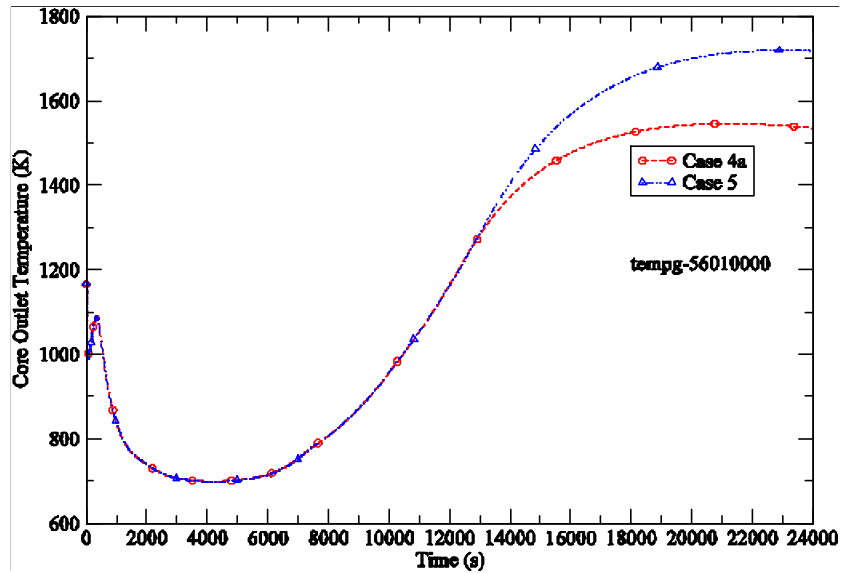


Figure 15 – Gas Temperature at Core Outlet.

### 5.2.8 Gas Temperature at Core Inlet

The initial surge in the core inlet temperature, shown in Figure 16, is somewhat unrealistic and is due to an approximation in the current PCU model discussed earlier in relation to the reactor pressure. In general the trend of the core inlet temperature corresponds to the difference between the heat removal rate of the emergency heat exchanger and reactor power. A positive differential implies a decrease in core inlet temperature and vice versa. The core inlet temperature is very similar for both cases and the general trend follows the ECS heat exchanger heat removal rate shown in Figure 9.

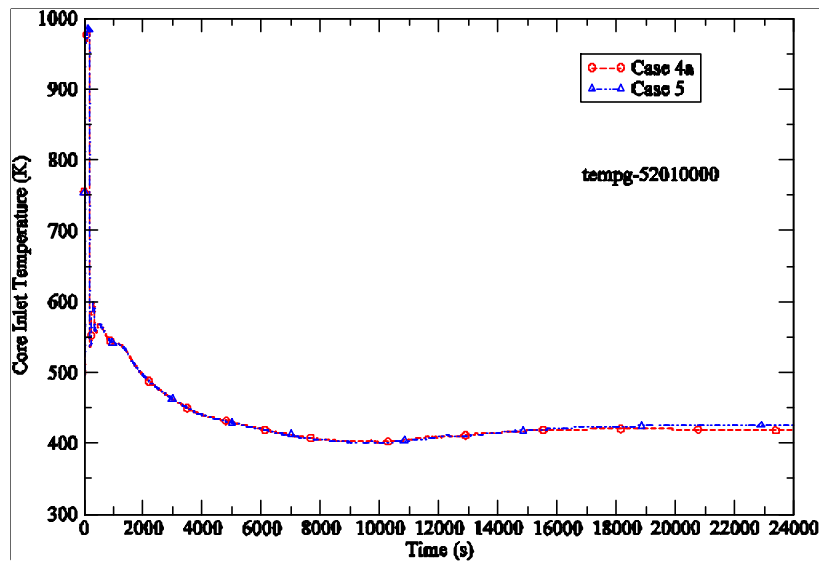


Figure 16 – Gas Temperature at Core Inlet.

## 6.0 SUMMARY AND CONCLUSIONS

An ATHENA model of a 2400MW GFR has been developed for the transient analysis of decay heat removal by natural circulation cooling. The model includes the passive emergency cooling system and the reactor cavity cooling system. Two modes of decay heat removal have been considered, namely convection and thermal radiation. Progress has also been made in the modeling of the turbo-machinery and heat exchangers of the power conversion unit.

Results of calculations using the ATHENA model have highlighted the effects of the guard containment back pressure on the maximum fuel temperature. A higher pressure leads to a higher natural circulation flow and a corresponding lower fuel temperature.

Heat structures and radiative heat transfer are important phenomena in the post-accident thermal progression of the core. The effect of including these phenomena is to re-distribute the radial temperature profile compared to not including them. Briefly, the hot zones (fuel) are reduced in temperature, and the cold zones (reflector, shield etc.) are increased in temperature relative to not including the above mentioned phenomena.

Results of analysis including the RCCS show that while the system is useful for lowering the guard containment pressure and temperature, its presence has a negative impact on the peak fuel temperature because the lower back pressure also reduces the natural circulation flow that removes most of the decay heat by convection. While the RCCS may be beneficial for other non-LOCA type accidents its impact in a depressurization accident would require further studies to evaluate the trade-offs. The same observation applies to other active or passive means of cooling the guard containment atmosphere. One example is the heat loss through the guard containment wall. Internal flow inside the guard containment tends to be quite complex and to correctly model the loss of heat by convection to the wall would require a more detailed analysis than what is possible with a system code.

The coolant flow due to the coast down of the Turbine-Compressor-Generator (TCG) unit is an important factor in initially cooling the core following a reactor scram and in establishing the natural circulation flow. Currently this flow is approximated by linearly reducing the flow velocity to zero in 180 seconds. A more realistic model of this flow reduction (both mass flow rate and time) is required to make more accurate estimates of the maximum fuel temperature, and ultimately the guard containment volume and pressure. In order to carry out this more realistic calculation a complete Turbine Compressor model is required and the modeling effort is in progress. This model will require the appropriate performance maps, inertia of the rotating parts, and some estimate of the internal friction of the blades rotating in the working fluid.

With a 100W/cc core power density the sensitivity of maximum fuel temperature to core power distribution has pointed to the need of a more uniform core power distribution radially and axially. Fuel pin design (pellet size, gap and clad thickness) also has a significant impact on the fuel temperature response in a depressurization accident.

## **7.0 REFERENCES**

- [1] Cheng, L., Ludewig, H. and Jo, J., “Passive Decay Heat Removal for a 2400 MW Pin Core by Natural Circulation,” BNL report submitted to the DOE GEN-IV Program, January 2005.
- [2] Cheng, L. and Ludewig, H., “Analysis Of Depressurization Accident for a 2400 MW Gas Cooled Reactor – Effects of the Reactor Cavity Cooling System,” BNL report submitted to the DOE GEN-IV Program, April 15 2005.
- [3] Cheng, L. and Ludewig, H., “Modeling of the Power Conversion Unit (PCU),” BNL report submitted to the DOE GEN-IV Program, July 15 2005.
- [4] Davis, C., Personal communication with L. Cheng (Electronic files related to major improvements made to the RELAP5-3D/ATHENA computer code for analysis of the GFR as part of an annual report (2004) for an INL LDRD), April 7, 2005.